arXiv:1609.06916v1 [cond-mat.str-el] 22 Sep 2016

Topological Gapless Phases in Non-Symmorphic Antiferromagnets

Wojciech Brzezicki[1] and Mario Cuoco[1]

[1] *CNR-SPIN and Dipartimento di Fisica "E. R. Caianiello", Università di Salerno, I-84084 Fisciano (Salerno), Italy*

Topologically protected fermionic quasiparticles occur in metals with band degeneracy as a consequence of band structure topology. Here we unveil topological semimetal and metal phases in a variety of non-symmorphic collinear antiferromagnets with glide reflection symmetry, a combination of mirror and half-lattice translation. We find gapless phases with Dirac points having multiple symmetry-protection as well as electronic structures with triple and quadruple band-crossing points. Glide semimetal is shown to be converted into a unique topological phase with non-trivial Z_2 topological charges at the Dirac points due to inversion and time-inversion symmetry combination. More striking is the emergence of a hidden non-unitary relation between the states in the glide sectors that provide a general mechanism to get multiple band touching points. The split Fermi points uncover a Z_2 protection that drives the changeover of the multiple-degenerate gapless phase into a topological metal built from their connection through distinct Fermi lines. Besides a new perspective of ordered states in complex materials, our findings indicate that novel topological gapless phases and edge states may occur in a wide class of magnetic systems.

PACS numbers: 73.22.-f,71.27.+a,03.65.Vf,75.50.Ee

a. Introduction – Topological materials have become the focus of intense research in the last years [1–4] not only for the perspective of new physical phenomena with potential technological applications, but also for being a test bed for fundamental concepts of physics theories. Along this line, recent efforts led to the theoretical prediction [5–8] and experimental realization [9–11] of topological insulators (TIs) in materials with strong spin-orbit coupling (SOC). One of the hallmarks of TIs is the existence of protected gapless edge states, which are due to a nontrivial topology of the bulk band structure. Such manifestation of topological order however is not limited to insulators as electronic structures with gapless topological modes have been predicted [12–20] and their relevance further boosted by the discovery of novel materials [21–26] with nontrivial band crossing points in the momentum space and robust edge states.

Among various kinds of topological matter, correlated materials with strong spin-orbital-charge entanglement, e.g. transition-metal oxides, represent a unique platform to explore topological effects combined to a large variety of intriguing collective properties emerging from electron-electron interaction, as superconductivity, magnetism, magnetoelectricity and Mott insulating phases. In these systems, complex magnetic orders generally arise from competing ferromagnetic (FM) and antiferromagnetic (AF) correlations with a frustrated localized-itinerant nature and a strong dependence on the orbital character of the transition metal d-shells. Magnetic patterns constructed by antiferromagnetically coupled zig-zag FM chains (Figs. 1(a),(b)) are one generic manifestation of such competing effects and often occur in the class of correlated materials as demonstrated in manganites [29–31], ruthenates [32–35], dichalcogenides [36–38], iridates [39, 40], nickelates [41–44], etc. A relevant mark of zig-zag patterns is the symmetry under non-symmorphic (NS) transformations that combine point group operations with translation that are a fraction of a Bravais lattice vector [28]. Recently, NS groups have been recognized as a new source of topological symmetry protection both in gapped [45–54] and gapless [55–60] systems. Hence, given the wide range of physical phenomena in both topological and correlated materials, the identification of novel topological phases in the presence of non trivial orderings and their material realizations set fundamental challenges in the condensed matter realm.

In this Letter, we unveil topological semimetal (SM) and metal phases in a variety of NS collinear antiferromagnets with glide reflection symmetry. The emergent topological gapless states can exhibit Dirac points (DPs) with multiple symmetry-protection as well as three- and four-fold spin-degenerate Fermi points. Besides NS symmetry protection, we demonstrate that inversion and combination of time-and-inversion can lead to non-trivial Z_2 topological charges at the DPs, thus building up a unique and robust topological SM phase. More striking is the occurrence of a hidden non-unitary relation between the states in the two glide sectors that provide a general mechanism to stick DPs or generate multiple band touching points in the glide plane (GP). We unveil how the splitting of the multiple degenerate Fermi points (FPs) drives the transition into a topological metal. Due to a Z_2 protection of the FPs in the glide plane, a topological metal arises with multiple Fermi pockets resulting from the Fermi lines connecting the FPs themselves.

b. Model and symmetries – We consider an effective orbital-directional model describing itinerant electrons (e.g. t_{2g} or p bands) in the presence of an anisotropic SOC, as due to tetragonal crystal field splitting, and Hund coupled to localized spin moments forming zig-zag pattern with characteristic length $L_z \geq 2$.

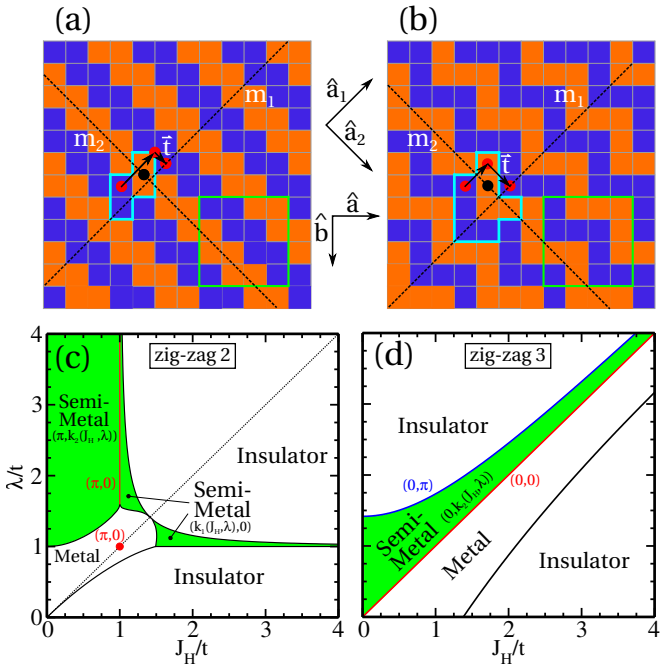

FIG. 1. Zigzag spin patterns with (a) length $L_z = 2$ ($z2$) and (b) $L_z = 3$ ($z3$). Orange and blue squares indicate spin-up and spin-down orientation. The unit cell is marked by a thick blue frame while $\hat{a}_{1,2}$ are the translation directions. The square unit cells are marked with green frames. Dashed lines indicate the normal mirror planes m_1 and m_2, with m_2 being related to the the gliding symmetry. The glide transformations is sketched via the red dots and arrows; the dot is subjected to the reflection m_2 then it is translated by a vector $\vec{t}$ parallel to the mirror plane m_2. For $z2$ these two steps separately do not reproduce the original lattice. The black dots are the inversion centers. Phase diagrams for (c) $z2$ at 3/4 filling and (d) $z3$ at half filling. Topological semimetal phases are marked with color (green area) and the position of Dirac points in the Brillouin zone is reported in brackets.

The model Hamiltonian is given by

$$\mathcal{H} = \sum_{i,\sigma} \sum_{\substack{\alpha,\beta=a,b \\ \hat{\gamma}=\hat{a},\hat{b}}} t_{\gamma,\alpha\beta} \left(d^{\dagger}_{i,\alpha\sigma} d_{i+\hat{\gamma},\beta\sigma} + h.c. \right)$$
$$- J_H \sum_{i,\alpha=a,b} s^z_{i\alpha} \cdot S^z_i + \lambda \sum_i S^z_i l^z_i \,,$$

where $d^{\dagger}_{i,\alpha\sigma}$ is the electron creation operator at the site i with spin σ for the orbital α, (a,b,c) are the (yz,xz,xy) orbitals which are perpendicular to the corresponding bond direction, with $\hat{a}$, $\hat{b}$, and $\hat{c}$ being the unit vectors along the lattice symmetry directions. α, $\mathbf{s}_{i\alpha} = d^{\dagger}_{i,\mu,\alpha} \sigma^z_{\alpha,\beta} d_{i,\mu,\beta}$ and $S^z_i = \pm 1$ denote the spins for the $d_{xz/yz}$ and d_{xy} orbitals, respectively. J_H stands for the Hund coupling, while λ is the SOC for the projected subspace of (a,b) orbitals, with $l^z_i = i \left(d^{\dagger}_{i,a,\sigma} d_{i,b,\sigma} - d^{\dagger}_{i,b,\sigma} d_{i,a,\sigma} \right)$ the z-component of the local angular momentum. $t_{\hat{\gamma},\alpha\beta}$ is the nearest-neighbor hopping amplitude between α and β for the bond along the $\hat{\gamma}$ direction. We assume $t_{\hat{a},bb} = t_{\hat{b},aa} = -t$ with t as energy scale unit. The AF states are collinear and the spin z-projection is a conserved quantity due to the anisotropic SOC. For the model in Eq. 1, the zig-zag states are the energetically most favorable configurations in a large range of doping concentration [27].

The relevant operations of NS groups in two dimensions are screw axis, glide mirror lines, and glide mirror planes in conjunction with the translation [28]. For zig-zag antiferromagnet (AFM), a NS glide transformation $\mathcal{R}^t$ can be constructed by the product of a reflection with respect to the m_2 plane and a translation $\vec{t} \equiv \vec{a}_2/2$ in the $\hat{a}_2$ direction along the zig-zag chain (Fig. 1). $\mathcal{R}^t$ includes spatial and orbital transformations. Indeed, the m_2 mirror interchanges the $\hat{a}$ and $\hat{b}$ lattice directions and consequently the orbitals. $\mathcal{R}^t$ is also intrinsically k-dependent as it is not possible to find a unit cell that maps onto itself under the glide transformation. By a proper choice of the unit cell or a suitable k-dependent transformation of $\mathcal{H}_{\vec{k}}$ one can show [61] that the glide operator depends only on k_2 as $\mathcal{R}^t_{k_2}$. We select a basis that makes $\mathcal{R}^t_{k_2}$ to have eigenvalues $g_{\pm} = \pm 1$ while the eigenvectors carry the k_2-dependence. As expected from the half-lattice translation of NS symmetry, the glide eigenstates have a larger periodicity in the momentum space. Apart from the glide $\mathcal{G}$, the model Hamiltonian has time reversal invariance, $\mathcal{T}$, chiral symmetry $\mathcal{S}$ at half-filling, as well as a normal reflection plane (m_1), and inversion centers associated to the normal mirror and inversion symmetry ($\mathcal{I}$) transformations.

Concerning the electronic behavior of zig-zag AFM, we focus on $z2$ and $z3$ magnetic patterns which are those more relevant for the realistic materials. A generic feature of the phase diagram, arising from the interplay of SOC and Hund exchange, is the presence of wide regions in the parameters space where topologically nontrivial SM phases occur in between the metallic and insulating regimes as demonstrated for two representative electron densities in Figs. 1 (c),(d).

c. Multiple symmetry protection – Let us now demonstrate how glide, inversion, and time-reversal combination protect the DPs in $z2$ AFMs (Fig.2(a)). The resulting electronic spectra in Figs. 2 (b)-(e) directly provide evidence of a striking *topological resilience* of DPs and edge modes, being always present upon different symmetry broken configurations. To set the stage, let us consider the band structure in the GP at $k_1 = \pi$ (Fig. 1(g)). Since the glide $\mathcal{R}^t_{k_2}$ commutes with $\mathcal{H}_{\vec{k}}$, the electronic states can be labeled by $g_{\pm}$ glide eigenvalues. The DPs occur at the crossing of the bands with opposite g and they are protected by an MZ mirror Chern number [62], taking values ± 1 for the two DPs, respectively. Furthermore, we find that in the one-dimensional (1D) cuts at any given k_2 the system has an inversion topological number $Z_>$ [65], with the inversion symmetry expressed by $\mathcal{R}^t_{k_2}$. $Z_>$ is defined as the difference of the number of occupied states with a chosen inversion eigenvalue at the two inversion invariant points, $k_1 = 0$ and $k_1 = \pi$ [61].

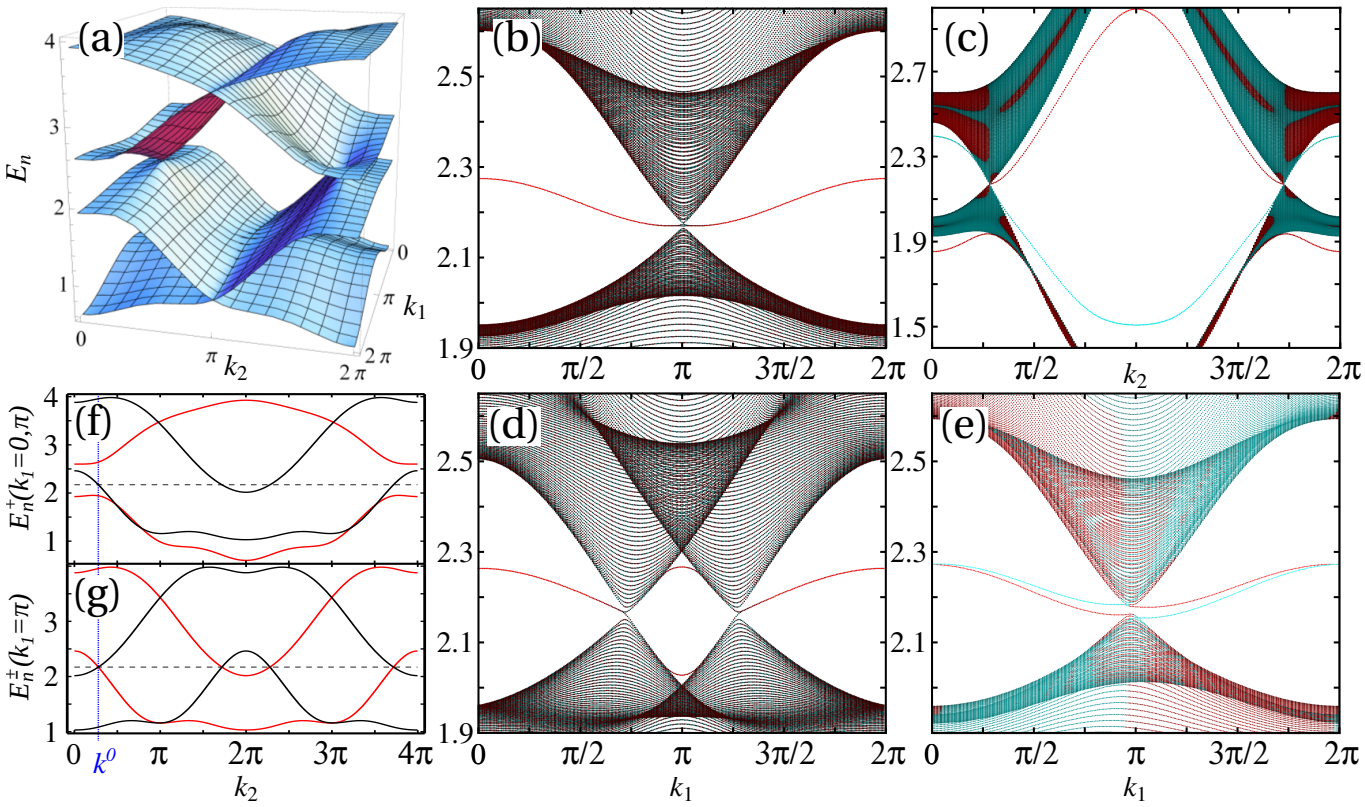

FIG. 2. Electronic spectra for $z2$ AF at 3/4 filling. (a) Bulk energy spectrum above zero energy. (b)-(e) one-dimensional spectra and edge states for a slab geometry with open boundary. Spectra for a slab configuration with open boundary in the (b) $\hat{a}_1$ and (c) $\hat{a}_2$ directions, with k_2 and k_1 being the momentum parallel to the edge, respectively. Electronic spectra with (d) open boundary along $\hat{a}_2$, broken glide and reflection symmetries with inversion invariance, and (e) with only broken time-reversal. (f) g_+ glide symmetric bands at $k_1 = 0$ (red) and $k_1 = \pi$ (black) as functions of k_2. (g) Band structure in the glide plane at $k_1 = \pi$, with glide eigenvalues $+1$ (red) and -1 (black). Dashed line sets the Fermi level. Color map of the spectra in (b)-(e) with high (low) brightness indicates a large (small) probability of the electronic states to be localized on the left (red) or right (blue) boundary.

Taking the spectra in the g_+ glide sector at $k_1 = \{0, \pi\}$, one can immediately deduce that $Z_>$ changes sign at the position of the DPS, i.e. k^0 and $2\pi - k^0$. The inversion symmetry protection of the DPs explains the presence of a third edge state close to the zone boundary in Fig. 2(c). In the absence of glide symmetry, $Z_>$ is meaningful only in the two high-symmetry cuts of the BZ, i.e. $k_2 = \{0, \pi\}$, and it is non-trivial at $k_2 = 0$ but trivial at $k_2 = \pi$, so there must be gap closings between these two 1D cuts (Fig. 1(f)). The last symmetry protection arises from the combination of $\mathcal{I}$ and $\mathcal{T}$. Their product yields a conjugation operator, $\mathcal{K}_{\vec{k}} \equiv \mathcal{I}_{\vec{k}}\mathcal{T}$, since $\mathcal{K}$ transforms $\mathcal{H}_{\vec{k}}$ into $\mathcal{H}^T_{\vec{k}}$. If $\mathcal{K}_{\vec{k}}\mathcal{K}^\star_{\vec{k}} \equiv 1$ (which is satisfied for any L_z) then $\mathcal{H}$ can be made purely real in the eigenbasis of $\mathcal{K}_{\vec{k}}$ [61]. Thus, close to the DPs, the low energy Hamiltonian has a form $H_{\delta\vec{k}} = \delta k_1 A + \delta k_2 B$ with A and B being 2×2 real symmetric matrices and $\delta\vec{k}$ the deviation with respect to the DP. Such Hamiltonian is in the class D of the Altland-Zinbauer table and for a Fermi surface with codimension $p = 2$ the system can be topological non-trivial with a Z_2 invariant [62]. The evaluation of $Z_2^{(1)}$ charge [61] indeed confirms that the DPs have Z_2 charges with values ± 1.

Concerning the lowering symmetry perturbations, breaking of glide in such a way that inversion is not preserved opens a gap and the system becomes topologically trivial whereas breaking of reflection or time only removes the Z_2 protection but leaves the glide protection so that the DPs are preserved. In Fig. 2(e) the case of time-reversal violation is considered. Due to a termination dependent orbital polarization, non-degenerate chiral states emerge at the edge and, remarkably, the system allows for non-vanishing charge and orbital currents at the boundary.

d. Multiple Fermi points and topological metal– The gapless phases in the GPs for $z3$ AFM exhibit quadruple and triple band touchings at half-filling and away from it (Figs. 3(a),(b)). The multiplicity of the Fermi points is not accidental. They appear in the GPs because of a *hidden* non-unitary relation that manifests itself on the level of determinant of the glide-block Hamiltonian. Indeed, for the Hamiltonian projected in the GP the two blocks are related by a 2π

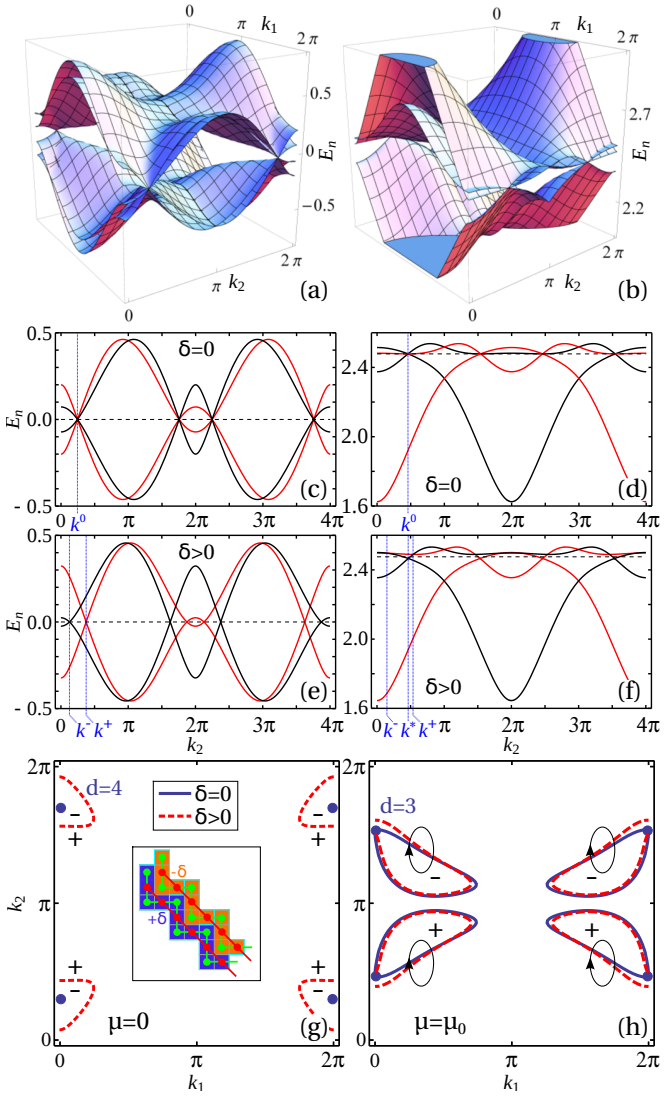

FIG. 3. Multiple Fermi points in $z3$ antiferromagnet. (a) bands with chiral four-fold DPs at half filling ($\mu = 0$), (b) bands with three-fold Fermi points at higher filling ($\mu = \mu_0$). (c), (d) the same bands in the glide plane $k = 0$ with color indicating the glide eigenvalue $+1$ (red) and -1 (black). Dashed line is the Fermi level μ. (e), (f) as in (c) and (d) plus a symmetry conserving long-range hopping δ. (g), (h) Fermi surfaces containing multiple Fermi points at $\delta = 0$ (blue) and $\delta > 0$ (red dashed). Multiple band crossing points are marked with dots and their degeneracy is indicated. The inset of (g) shows a schematic view of the hopping δ. The signs in (g) indicate the band parity, $+1$ inside the Fermi pockets and -1 outside. The signs in (h) are those due the AI winding numbers of the Fermi lines. The integration contours are indicated by ellipses.

shift, i.e., $H^{+}_{0,k_2} = H^{-}_{0,k_2+2\pi}$. However, while the spectrum of H^{+}_{0,k_2} is 4π-periodic, its determinant has a 2π-periodicity, $\det(\mathrm{H}^{+}_{0,\mathrm{k}_2} - \mu) \equiv \det(\mathrm{H}^{+}_{0,\mathrm{k}_2+2\pi} - \mu)$, at $\mu = 0$ and $\mu = \mu_0 = \sqrt{2 + J_H^2 + \lambda^2}$, for the case of chiral and non-chiral DPs, respectively. Such feature seems to be a remnant of the original periodicity of the full Hamiltonian and it implies that a μ eigenvalue of H^{+}_{0,k_2} must be 2π periodic. Then, (i) the 2π-shift relation of the glide symmetric blocks and (ii) the 2π-periodic determinant combine to glue together DPs from different glide-blocks at two specific energy levels, $\mu = 0, \mu_0$. We note that while such property is similar to the *congruence*, it turns out not to be exactly equivalent. Indeed, a hermitian congruence is found between the blocks H^{+}_{0,k_2} and $H^{+}_{0,k_2+2\pi}$, thus meaning that in a given basis these blocks differ only by a scaling of the rows and columns entries [66]. The anomalous periodicity of the determinant can be constructed explicitly [61] through a non-unitary chiral-like operator $\Sigma_{k_2} \equiv h^{-1}_{k_2} \bar{H}_{k_2}$ where $\bar{H}_{k_2}$ is the 2π periodic part of H^{+}_{0,k_2} and h_{k_2} is the part with 4π period ($h_{k_2+2\pi} \equiv -h_{k_2}$). The proof relies on the fact that eigenvalues of Σ_{k_2} are symmetric around zero and on the Silverster property of determinants, i.e., $\det(1 + \mathrm{AB}) \equiv \det(1 + \mathrm{BA})$. The emergence of a non-unitary relation that leaves the determinant invariant is a novel mechanism for the search and generation of multiple band touching points in the presence of NS symmetries.

Though the multiple band crossing points are not topological protected, they contain a topological character that marks the metallic phase. By adding a symmetry conserving second and third nearest-neighbors hopping (δ) the degeneracy is removed and the DPs are split (Figs. 3(e),(f)). The removal of the degeneracy is concomitant with a transition from semimetal to metal whose Fermi surface is, however, dictated by the presence of topological protected DPs in the glide plane due to band crossing in each glide sector. At $\mu = 0$, the Z_2 number associated to the Fermi pockets and the DPs in the glide plane can be directly obtained from the chiral and conjugation symmetries. Indeed, by introducing the anticonjugation operator $\mathcal{A}_{\vec{k}} = \mathcal{S}_{k_1}\mathcal{K}_{\vec{k}}$, acting like a particle-hole transformation at a high-symmetry point, one can show that if $\mathcal{A}_{\vec{k}}\mathcal{A}^{\star}_{\vec{k}} \equiv 1$, holding only for odd L_z, then $\mathcal{H}_{\vec{k}}$ can be made purely imaginary and thus antisymmetric in the eigenbasis of $\mathcal{A}_{\vec{k}}$. For the antisymmetric $\mathcal{H}_{\vec{\parallel}}$ the Z_2 number is defined by its Pfaffian and the Fermi pockets manifest themselves as the locus of points where the Pfaffian changes sign and band inversion occurs (Fig. 3 (g)). Hence, the metal phase is marked by two Fermi pockets that are glued to the glide plane through the topological protected DPs at $k_1 = 0$. Away from half-filling, e.g. at $\mu = \mu_0$, the triple band crossing is already coexisiting with a Fermi pocket (Fig. 3 (e)) and the removal of the degeneracy leads to topological protected DPs in the glide plane due to the combination of inversion and time as for the $z2$ pattern. The resulting metal phase is made of Fermi lines that also exhibit a non trivial AI winding number [61].

The realization of topological zig-zag AFMs and anomalous edge states has been so far focusing on specific insulating configurations [67–69]. Our analysis demonstrates that multi-orbital zig-zag AFMs, due to the NS symmetry, generally lead to topological gapless phases

whose nature depend on the characteristic zig-zag length as well as on the intricate entanglement of NS and internal or other spatial symmetries. The emergent invariance of the determinants in the glide sectors is a novel mechanism, uniquely arising in NS systems, to generate multiple band touching Fermi points and consequently topological non-trivial gapless phases.

Acknowledgements W.B. acknowledges support by the European Horizon 2020 research and innovation programme under the Marie-Sklodowska-Curie grant agreement No. 655515.

I. APPENDIX

A. Stucture of the Hamiltonian for $L_z = 2$ and $L_z = 3$ zigzag patterns

The general form of the Hamiltonian in Eq. 1 (see the main text) for a zigzag spin pattern can be obtained by analyzing the possible hopping processes for a given unit cell, as shown in Fig. 1 (see the main text). Its matrix representation for a given quasimomentum $\vec{k}$ and fixed spin polarization of the itinerant electrons, that is a good quantum number, can be conveniently written by a block matrix of the form,

$$\mathcal{H}_{\vec{k}} = \begin{pmatrix} \mathbf{H}^{bb}_{\downarrow\downarrow} & \mathbf{H}^{bb}_{\downarrow\uparrow} & \mathbf{H}^{ba}_{\downarrow\downarrow} & \mathbf{H}^{ba}_{\downarrow\uparrow} \\ \mathbf{H}^{bb}_{\uparrow\downarrow} & \mathbf{H}^{bb}_{\uparrow\uparrow} & \mathbf{H}^{ba}_{\uparrow\downarrow} & \mathbf{H}^{ba}_{\uparrow\uparrow} \\ \mathbf{H}^{ab}_{\downarrow\downarrow} & \mathbf{H}^{ab}_{\downarrow\uparrow} & \mathbf{H}^{aa}_{\downarrow\downarrow} & \mathbf{H}^{aa}_{\downarrow\uparrow} \\ \mathbf{H}^{ab}_{\uparrow\downarrow} & \mathbf{H}^{ab}_{\uparrow\uparrow} & \mathbf{H}^{aa}_{\uparrow\downarrow} & \mathbf{H}^{aa}_{\uparrow\uparrow} \end{pmatrix}. \tag{1}$$

Here, the blocks $\mathbf{H}^{\alpha\beta}_{\sigma\sigma'}(\sigma,\sigma' =\uparrow,\downarrow$ and $\alpha,\alpha' = a,b)$ are of the size $N_\downarrow = N_\uparrow = 2L_z - 2$, being the size of the spin up/down domaind within the unite cell (see Fig. 1). The indices $(\sigma\alpha)$ and $(\sigma'\beta)$ mean that the block decsribes hopping from the spin σ to spin σ' domain between orbitals α and β. For $z2$ magnetic pattern these blocks for the electrons with spin up are given by the equations,

$$\mathbf{H}^{bb}_{\downarrow\downarrow} = \begin{pmatrix} J_H & -e^{-ik_2}t^{bb}_{\hat{a}} + t^{bb}_{\hat{b}} \\ -e^{ik_2}t^{bb}_{\hat{a}} + t^{bb}_{\hat{b}} & J_H \end{pmatrix}, \tag{2}$$

$$\mathbf{H}^{bb}_{\uparrow\uparrow} = \begin{pmatrix} -J_H & -e^{-ik_2}t^{bb}_{\hat{a}} + t^{bb}_{\hat{b}} \\ -e^{ik_2}t^{bb}_{\hat{a}} + t^{bb}_{\hat{b}} & -J_H \end{pmatrix}, \tag{3}$$

$$\mathbf{H}^{bb}_{\downarrow\uparrow} = \begin{pmatrix} 0 & e^{-ik_2}t^{bb}_{\hat{b}} - t^{bb}_{\hat{a}} \\ -e^{-ik_1}t^{bb}_{\hat{a}} + e^{i(k_2-k_1)}t^{bb}_{\hat{b}} & 0 \end{pmatrix}, \tag{4}$$

$$\mathbf{H}^{bb}_{\uparrow\downarrow} = \left(\mathbf{H}^{bb}_{\downarrow\uparrow}\right)^\dagger, \tag{5}$$

for the b-orbital sector and

$$\mathbf{H}^{aa}_{\downarrow\downarrow} = \begin{pmatrix} J_H & e^{-ik_2}t^{aa}_{\hat{a}} - t^{aa}_{\hat{b}} \\ e^{ik_2}t^{aa}_{\hat{a}} - t^{aa}_{\hat{b}} & J_H \end{pmatrix}, \tag{6}$$

$$\mathbf{H}^{aa}_{\uparrow\uparrow} = \begin{pmatrix} -J_H & e^{-ik_2}t^{aa}_{\hat{a}} - t^{aa}_{\hat{b}} \\ e^{ik_2}t^{aa}_{\hat{a}} - t^{aa}_{\hat{b}} & -J_H \end{pmatrix}, \tag{7}$$

$$\mathbf{H}^{aa}_{\downarrow\uparrow} = \begin{pmatrix} 0 & -e^{-ik_2}t^{aa}_{\hat{b}} + t^{aa}_{\hat{a}} \\ e^{-ik_1}t^{aa}_{\hat{a}} - e^{i(k_2-k_1)}t^{aa}_{\hat{b}} & 0 \end{pmatrix}, \tag{8}$$

$$\mathbf{H}^{aa}_{\uparrow\downarrow} = \left(\mathbf{H}^{aa}_{\downarrow\uparrow}\right)^\dagger, \tag{9}$$

for the a-orbital sector. For the interorbital sector we have,

$$\mathbf{H}^{ba}_{\downarrow\downarrow} = \begin{pmatrix} i\lambda & e^{-ik_2}t^{ab}_{\hat{a}} + t^{ab}_{\hat{b}} \\ -e^{ik_2}t^{ab}_{\hat{a}} - t^{ab}_{\hat{b}} & i\lambda \end{pmatrix}, \tag{10}$$

$$\mathbf{H}^{ba}_{\uparrow\uparrow} = \begin{pmatrix} -i\lambda & e^{-ik_2}t^{ab}_{\hat{a}} + t^{ab}_{\hat{b}} \\ -e^{ik_2}t^{ab}_{\hat{a}} - t^{ab}_{\hat{b}} & -i\lambda \end{pmatrix}, \tag{11}$$

$$\mathbf{H}^{ba}_{\downarrow\uparrow} = \begin{pmatrix} 0 & e^{-ik_2}t^{ab}_{\hat{b}} + t^{ab}_{\hat{a}} \\ -e^{-ik_1}t^{ab}_{\hat{a}} - e^{i(k_2-k_1)}t^{ab}_{\hat{b}} & 0 \end{pmatrix}, \tag{12}$$

$$\mathbf{H}^{ba}_{\uparrow\downarrow} = \begin{pmatrix} 0 & e^{ik_1}t^{ab}_{\hat{a}} + e^{i(k_1-k_2)}t^{ab}_{\hat{b}} \\ -e^{ik_2}t^{ab}_{\hat{b}} - t^{ab}_{\hat{a}} & 0 \end{pmatrix}, \tag{13}$$

and the rest of blocks can be recovered from these as

$$\mathbf{H}^{ab}_{\sigma\sigma'} = \left(\mathbf{H}^{ba}_{\sigma'\sigma}\right)^\dagger. \tag{14}$$

We note that here the spin sectors for the itinerat electrons are completely equivalent. We can obtain the Hamiltonian blocks for the opposite sector by changing the sign of J_H and λ. For zig-zag $z3$ the size of the spin domain is $N_\downarrow = 4$ so that the blocks are twice larger. Then, we have

$$\mathbf{H}^{bb}_{\downarrow\downarrow} = \begin{pmatrix} J_H & t^{bb}_{\hat{b}} & 0 & -e^{-ik_2}t^{bb}_{\hat{a}} \\ t^{bb}_{\hat{b}} & J_H & t^{bb}_{\hat{b}} & 0 \\ 0 & t^{bb}_{\hat{b}} & J_H & -t^{bb}_{\hat{a}} \\ -e^{ik_2}t^{bb}_{\hat{a}} & 0 & -t^{bb}_{\hat{a}} & J_H \end{pmatrix}, \tag{15}$$

$$\mathbf{H}^{bb}_{\uparrow\uparrow} = \begin{pmatrix} -J_H & t^{bb}_{\hat{b}} & 0 & -e^{-ik_2}t^{bb}_{\hat{a}} \\ t^{bb}_{\hat{b}} & -J_H & t^{bb}_{\hat{b}} & 0 \\ 0 & t^{bb}_{\hat{b}} & -J_H & -t^{bb}_{\hat{a}} \\ -e^{ik_2}t^{bb}_{\hat{a}} & 0 & -t^{bb}_{\hat{a}} & -J_H \end{pmatrix}, \tag{16}$$

$$\mathbf{H}^{bb}_{\downarrow\uparrow} = N_\downarrow \begin{pmatrix} 0 & -t^{bb}_{\hat{a}} & 0 & e^{-ik_2}t^{bb}_{\hat{b}} \\ -e^{-ik_1}t^{bb}_{\hat{a}} & 0 & -t^{bb}_{\hat{a}} & 0 \\ 0 & -e^{-ik_1}t^{bb}_{\hat{a}} & 0 & e^{-ik_1}t^{bb}_{\hat{b}} \\ e^{i(k_2-k_1)}t^{bb}_{\hat{b}} & 0 & t^{bb}_{\hat{b}} & 0 \end{pmatrix} \tag{17}$$

$$\mathbf{H}^{bb}_{\uparrow\downarrow} = \left(\mathbf{H}^{bb}_{\downarrow\uparrow}\right)^\dagger, \tag{18}$$

for the b-orbital sector, and

$$\mathbf{H}^{aa}_{\downarrow\downarrow} = \begin{pmatrix} J_H & -t^{aa}_{\hat{b}} & 0 & e^{-ik_2}t^{aa}_{\hat{a}} \\ -t^{aa}_{\hat{b}} & J_H & -t^{aa}_{\hat{b}} & 0 \\ 0 & -t^{aa}_{\hat{b}} & J_H & t^{aa}_{\hat{a}} \\ e^{ik_2}t^{aa}_{\hat{a}} & 0 & t^{aa}_{\hat{a}} & J_H \end{pmatrix}, \tag{19}$$

$$\mathbf{H}^{aa}_{\uparrow\uparrow} = \begin{pmatrix} -J_H & -t^{aa}_{\hat{b}} & 0 & e^{-ik_2}t^{aa}_{\hat{a}} \\ -t^{aa}_{\hat{b}} & -J_H & -t^{aa}_{\hat{b}} & 0 \\ 0 & -t^{aa}_{\hat{b}} & -J_H & t^{aa}_{\hat{a}} \\ e^{ik_2}t^{aa}_{\hat{a}} & 0 & t^{aa}_{\hat{a}} & -J_H \end{pmatrix}, \tag{20}$$

$$\mathbf{H}^{aa}_{\downarrow\uparrow} = \begin{pmatrix} 0 & t^{aa}_{\hat{a}} & 0 & -e^{-ik_2}t^{aa}_{\hat{b}} \\ e^{-ik_1}t^{aa}_{\hat{a}} & 0 & t^{aa}_{\hat{a}} & 0 \\ 0 & e^{-ik_1}t^{aa}_{\hat{a}} & 0 & -e^{-ik_1}t^{aa}_{\hat{b}} \\ -e^{i(k_2-k_1)}t^{aa}_{\hat{b}} & 0 & -t^{aa}_{\hat{b}} & 0 \end{pmatrix} \tag{21}$$

$$\mathbf{H}^{aa}_{\uparrow\downarrow} = \left(\mathbf{H}^{aa}_{\downarrow\uparrow}\right)^{\dagger}, \tag{22}$$

for the a-orbital sector. For the interorbital sector we have

$$\mathbf{H}^{ba}_{\downarrow\downarrow} = \begin{pmatrix} i\lambda & t^{ab}_{\hat{b}} & 0 & e^{-ik_2}t^{ab}_{\hat{a}} \\ -t^{ab}_{\hat{b}} & i\lambda & -t^{ab}_{\hat{b}} & 0 \\ 0 & t^{ab}_{\hat{b}} & i\lambda & t^{ab}_{\hat{a}} \\ -e^{ik_2}t^{ab}_{\hat{a}} & 0 & -t^{ab}_{\hat{a}} & i\lambda \end{pmatrix}, \tag{23}$$

$$\mathbf{H}^{ba}_{\uparrow\uparrow} = \begin{pmatrix} -i\lambda & t^{ab}_{\hat{b}} & 0 & e^{-ik_2}t^{ab}_{\hat{a}} \\ -t^{ab}_{\hat{b}} & -i\lambda & -t^{ab}_{\hat{b}} & 0 \\ 0 & t^{ab}_{\hat{b}} & -i\lambda & t^{ab}_{\hat{a}} \\ -e^{ik_2}t^{ab}_{\hat{a}} & 0 & -t^{ab}_{\hat{a}} & -i\lambda \end{pmatrix}, \tag{24}$$

$$\mathbf{H}^{ba}_{\downarrow\uparrow} = \begin{pmatrix} 0 & t^{ab}_{\hat{a}} & 0 & e^{-ik_2}t^{ab}_{\hat{b}} \\ -e^{-ik_1}t^{ab}_{\hat{a}} & 0 & -t^{ab}_{\hat{a}} & 0 \\ 0 & e^{-ik_1}t^{ab}_{\hat{a}} & 0 & e^{-ik_1}t^{ab}_{\hat{b}} \\ -e^{i(k_2-k_1)}t^{ab}_{\hat{b}} & 0 & -t^{ab}_{\hat{b}} & 0 \end{pmatrix}, \tag{25}$$

$$\mathbf{H}^{ba}_{\uparrow\downarrow} = \begin{pmatrix} 0 & e^{ik_1}t^{ab}_{\hat{a}} & 0 & e^{i(k_1-k_2)}t^{ab}_{\hat{b}} \\ -t^{ab}_{\hat{a}} & 0 & -e^{ik_1}t^{ab}_{\hat{a}} & 0 \\ 0 & t^{ab}_{\hat{a}} & 0 & t^{ab}_{\hat{b}} \\ -e^{ik_2}t^{ab}_{\hat{b}} & 0 & -e^{ik_1}t^{ab}_{\hat{b}} & 0 \end{pmatrix} \tag{26}$$

and the remaining blocks are as in Eq. (14)

$$\mathbf{H}^{ab}_{\sigma\sigma'} = \left(\mathbf{H}^{ba}_{\sigma'\sigma}\right)^{\dagger}.$$

B. Reducing the Hamiltonian into a purely real matrix form

The combination of the time reversal and inversion transformation leads to the operator $\mathcal{K}_{\vec{k}}$ defined as,

$$\mathcal{K}_{\vec{k}} \equiv \mathcal{I}_{\vec{k}}\mathcal{T}, \tag{27}$$

whose action on the Hamiltonian is to make it transposed or complex conjugated,

$$\mathcal{K}^{\dagger}_{\vec{k}}\mathcal{H}_{\vec{k}}\mathcal{K}_{\vec{k}} = \mathcal{H}^{T}_{\vec{k}}. \tag{28}$$

Thus, we can generally indicate $\mathcal{K}_{\vec{k}}$ as a *conjugation* operator. Due to its structure and on the property of $\mathcal{I}$ and $\mathcal{T}$, we find that the square of $\mathcal{K}_{\vec{k}}$ gives the identity, i.e.,

$$\mathcal{K}_{\vec{k}}\mathcal{K}^{\star}_{\vec{k}} \equiv 1\,. \tag{29}$$

From the fact that $\mathcal{K}_{\vec{k}}$ is unitary, we also deduce that $\mathcal{K}_{\vec{k}} = \exp(iK_{\vec{k}})$, where $K_{\vec{k}}$ is a hermitian matrix. Thus, if $\mathcal{K}_{\vec{k}}\mathcal{K}^{\star}_{\vec{k}} \equiv 1$ then $K_{\vec{k}}$ must be also symmetric and real. On this basis, $K_{\vec{k}}$ can be diagonalized by a real unitary transformation and accordingly for $\mathcal{K}_{\vec{k}}$. The eigenvalues of $\mathcal{K}_{\vec{k}}$ are ± 1, hence it can be put in a diagonal form $\mathcal{D}_{\mathcal{K}}$ by a suitable unitary and *real* transformation $\mathcal{U}_{\vec{k}}$:

$$\mathcal{D}_{\mathcal{K}} \equiv \mathcal{U}^{\dagger}_{\vec{k}}\mathcal{K}_{\vec{k}}\mathcal{U}_{\vec{k}} = \begin{pmatrix} \mathbf{1} & \mathbf{0} \\ \mathbf{0} & -\mathbf{1}\,. \end{pmatrix}, \tag{30}$$

Furthermore, we can introduce another unitary transformation $\mathcal{V}_{\vec{k}}$ as

$$\mathcal{V}_{\vec{k}} \equiv \mathcal{U}_{\vec{k}}\sqrt{\mathcal{D}_{\mathcal{K}}}, \tag{31}$$

in such a way that we can transform the Hamiltonian to get $\mathcal{H}'_{\vec{k}}$ in the following form

$$\mathcal{H}'_{\vec{k}} = \mathcal{V}^{\dagger}_{\vec{k}}\tilde{\mathcal{H}}_{\vec{k}}\mathcal{V}_{\vec{k}}. \tag{32}$$

It is then important to notice that the transformed Hamiltonian is purely real. To achieve this result one needs to transform $\tilde{\mathcal{K}}$ by means of $\tilde{\mathcal{V}}$, recalling that $\tilde{\mathcal{K}}$ transforms as an anti-unitary operator. Indeed, one obtains

$$\mathcal{K}'_{\vec{k}} = \mathcal{V}^{T}_{\vec{k}}\mathcal{K}_{\vec{k}}\mathcal{V}_{\vec{k}}, \tag{33}$$

and from the definition of $\mathcal{V}_{\vec{k}}$ and from the fact that $\mathcal{U}_{\vec{k}}$ is real we get

$$\mathcal{K}'_{\vec{k}} = 1. \tag{34}$$

On the other hand, since we know that $\mathcal{K}'$ satisfies a relation with $\mathcal{H}'_{\vec{k}}$ which is given

$$(\mathcal{K}'_{\vec{k}})^{\dagger}\mathcal{H}'_{\vec{k}}\mathcal{K}'_{\vec{k}} = (\mathcal{H}'_{\vec{k}})^{T}. \tag{35}$$

we finally conclude that $\mathcal{H}'_{\vec{k}} \equiv (\mathcal{H}'_{\vec{k}})^{T}$ that implies $\mathcal{H}'_{\vec{k}}$ to be purely real.

C. Determinant equivalence of the glide blocks

1. *Half-filling case*

Taking the two glide plane Hamiltonians $\mathcal{H}_{0,k_2}$ and $\mathcal{H}_{\pi,k_2}$ we can use the eigenbasis $\mathcal{V}_{k_2}$ of the glide operator $\mathcal{R}^{t}_{k_2}$ to make it block-diagonal as

$$\mathcal{H}'_{0(\pi),k_2} \equiv \mathcal{V}^{\dagger}_{k_2}\mathcal{H}_{0(\pi),k_2}\mathcal{V}_{k_2} = \begin{pmatrix} H^{+}_{0(\pi),k_2} & 0 \\ 0 & H^{-}_{0(\pi),k_2} \end{pmatrix}, \tag{36}$$

where $H^{\pm}_{0(\pi),k_2}$ are the blocks of equal size in the subspaces of $+1$ and -1 eigenvalues of$\mathcal{R}^t_{k_2}$. One finds that these blocks are equal modulo 2π shift in k_2, that is

$$H^{\mp}_{0(\pi),k_2} = H^{\pm}_{0(\pi),k_2+2\pi}. \tag{37}$$

Note that 2π shift in k_2 is relevant from the point of view of $H^{\mp}_{0(\pi),k_2}$ because now we are in the eigenbasis of $\mathcal{R}^t_{k_2}$ which is k-dependent and the period of $H^{\mp}_{0(\pi),k_2}$ is twice elongated. This property, that holds for any zig-zag segment length L_z, implies that the whole spectrum of the glide-plane Hamiltonian is fully determined in just one eigen-subspace of the glide operator.

Now we will show that at *the same* k_2 the spectra of $H^{\mp}_{0(\pi),k_2}$ are related in a very special way. Namely, for any L_z and $k_1 = 0$ we find that,

$$\det H^{+}_{0,k_2} \equiv \det H^{-}_{0,k_2} \equiv \det H^{+}_{0,k_2+2\pi}, \tag{38}$$

and for any *odd* L_z and $k_1 = \pi$ we have,

$$\det H^{+}_{\pi,k_2} \equiv \det H^{-}_{\pi,k_2} \equiv \det H^{+}_{\pi,k_2+2\pi}. \tag{39}$$

This means that in each block the product of all eigenvalues is 2π periodic although these eigenvalues by themselves have longer period.

Let us show why such property of determinant holds by considering zig-zag patterns with $L_z = 3$ and $k_1 = 0$. We find the determinant of a glide block to be,

$$\det H^{+}_{0,k_2} = \left(-2 + \left(J_H^2 - \lambda^2\right)^2 + 2\cos k_2\right)^2, \tag{40}$$

although the periodicity of H^{+}_{0,k_2} is 4π.

Such relation is related to a sort of *hidden* symmetry. Indeed, the block can be written in the following way

$$H^{+}_{0,k_2} = h_{k_2} + \bar{H}_{k_2}, \tag{41}$$

where $\bar{H}_{k_2}$ is the 2π periodic part of H^{+}_{0,k_2}, i.e., $\bar{H}_{k_2+2\pi} \equiv \bar{H}_{k_2}$ and h_{k_2} is the part with 4π period. Since the dependence on k_2 is always enclosed in sine and cosine type functions we have

$$h_{k_2+2\pi} \equiv -h_{k_2}. \tag{42}$$

Now, we can write the desired determinant in the following way,

$$\det H^{+}_{0,k_2} = \det\left(h_{k_2} + \bar{H}_{k_2}\right) = \det h_{k_2} \det\left(1 + \Sigma_{k_2}\right), \tag{43}$$

where $\Sigma_{k_2} \equiv h^{-1}_{k_2}\bar{H}_{k_2}$. This step requires h_{k_2} to be an invertible function, and it holds because h_{k_2} has eigenvalues $\pm\lambda$ so it is non-singular for any k_2. The new operator Σ_{k_2} satisfies the relation $\Sigma_{k_2+2\pi} \equiv -\Sigma_{k_2}$. It is non-hermitian and in principle can be non-diagonalizable. In our case, we find Σ_{k_2} to be diagonalizable and its spectrum to be chiral with the following eigenvalues

$$s_{k_2} = \pm\frac{1}{\lambda}\sqrt{J_H^2 \pm 2\sin\frac{k_2}{2}}, \tag{44}$$

and being double degenerate. This means that there exist a non-singular operator β_{k_2} that anticommutes with Σ_{k_2} namely

$$\{\beta_{k_2}, \Sigma_{k_2}\} \equiv 0. \tag{45}$$

Using this property we can prove that determinant of H^{+}_{0,k_2} is 2π periodic as

$$\det H^{+}_{0,k_2+2\pi} = (-1)^{N_\downarrow} \det h_{k_2} \det\left(1 - \Sigma_{k_2}\right). \tag{46}$$

Then, we focus on the second term and the anticommutation of β_{k_2},

$$\det\left(1 - \beta^{-1}_{k_2}\beta_{k_2}\Sigma_{k_2}\right) = \det\left(1 + \beta^{-1}_{k_2}\Sigma_{k_2}\beta_{k_2}\right),$$

as well as we take into account the Silvester identity that sets the relation between the determinants of two generic matrices A and B

$$\det\left(1 + AB\right) = \det\left(1 + BA\right). \tag{47}$$

Choosing $A = \beta^{-1}_{k_2}\Sigma_{k_2}$ and $B = \beta_{k_2}$ we finally have that,

$$\det\left(1 + \beta^{-1}_{k_2}\Sigma_{k_2}\beta_{k_2}\right) = \det\left(1 + \Sigma_{k_2}\right), \tag{48}$$

and thus

$$\det\left(1 - \Sigma_{k_2}\right) = \det\left(1 + \Sigma_{k_2}\right). \tag{49}$$

This implies that

$$\det H^{+}_{0,k_2+2\pi} = (-1)^{N_\downarrow} \det H^{+}_{0,k_2}. \tag{50}$$

Since $N_\downarrow$ is always even in our zig-zag patterns we succeed in demonstrating that the determinant of the glide block is indeed 2π periodic. We point out that a crucial ingredient for the proof is given by the existence of an *invertible* operator β_{k_2} that anticommutes with Σ_{k_2}. We found that such chirality also occurs for $k = \pi$ glide plane and for other zig-zag segment lengths L_z.

2. *Away from half-filling*

The property of determinat of a glide block described in the previous Section can be more general in case of some L_z. Namely, we can find such values of chemical potential μ that a following relation is satisfied,

$$\det\left(H^{+}_{0,k_2} - \mu\right) \equiv \det\left(H^{+}_{0,k_2+2\pi} - \mu\right). \tag{51}$$

In case of zig-zag $L_z = 3$ we find that there is one non-trivial value of μ satisfying this relation,

$$\mu_0 = \pm\sqrt{2 + J_H^2 + \lambda^2}, \tag{52}$$

where the freedom of sign comes from the chirality of H^{+}_{0,k_2}. The determinant then becomes,

$$\det\left(H^{+}_{0,k_2}-\mu_0\right)=4\left(1-2J_H^2\lambda^2+\cos k_2\right)^2. \quad (53)$$

So indeed it is 2π periodic. Why it happens we can prove in a indirect way. We define a chiral-square block $H^{+(2)}_{0,k_2}$ as,

$$H^{+(2)}_{\mu,k_2}\equiv (H^{+}_{0,k_2})^2-\mu^2. \quad (54)$$

For this block we can prove using the method from the previous section that,

$$\det H^{+(2)}_{\mu,k_2}=\det H^{+(2)}_{\mu,k_2+2\pi}. \quad (55)$$

Now having this we can relate the determinant of $H^{+(2)}_{\mu,k_2}$ with determinant of $(H^{+}_{0,k_2}-\mu)$ (modulo sign) in a following way,

$$\begin{aligned}\det H^{+(2)}_{\mu,k_2}&=\det\left(H^{+}_{0,k_2}+\mu\right)\det\left(H^{+}_{0,k_2}-\mu\right)\\&=(-1)^{N_\downarrow}\det\left(H^{+}_{0,k_2}-\mu\right)^2, \quad (56)\end{aligned}$$

where for the second equality we used the chirality operator of H^{+}_{0,k_2} and the Silvester identity of Eq. (47) in the same way as we did in previous section for Σ_{k_2} and β_{k_2}.

The prove of property (55) can be done in way described in the previous Section. First we decompose $H^{+(2)}_{\mu,k_2}$,

$$H^{+(2)}_{\mu,k_2}=h^{(2)}_{k_2}+\bar{H}^{(2)}_{\mu,k_2}, \quad (57)$$

into the part which is 2π periodic - $\bar{H}^{(2)}_{\mu,k_2}$ and the rest, $h^{(2)}_{k_2}$ satisfying $h^{(2)}_{k_2+2\pi}\equiv -h^{(2)}_{k_2}$. Now we define the operator $\Sigma^{(2)}_{\mu,k_2}$ which we would like to be chiral, i.e.,

$$\Sigma^{(2)}_{\mu,k_2}\equiv h^{(2)-1}_{k_2}\bar{H}^{(2)}_{\mu,k_2}. \quad (58)$$

Indeed the spectrum of $\Sigma^{(2)}_{\mu,k_2}$ is chiral if only $\mu=\mu_0$ but there is one subtelty here - $\Sigma^{(2)}_{\mu_0,k_2}$ is non-diagonalizable (defective). We find that it has a non-trivial Jordan form given by,

$$\Sigma^{(2)'}_{\mu_0,k_2}=\begin{pmatrix}-s_{k_2}&1&0&0&0&0&0&0\\0&-s_{k_2}&0&0&0&0&0&0\\0&0&-s_{k_2}&1&0&0&0&0\\0&0&0&-s_{k_2}&0&0&0&0\\0&0&0&0&s_{k_2}&0&0&0\\0&0&0&0&0&s_{k_2}&0&0\\0&0&0&0&0&0&s_{k_2}&0\\0&0&0&0&0&0&0&s_{k_2}\end{pmatrix}, \quad (59)$$

with eigenvalues,

$$\pm\, s_{k_2}\equiv\pm\frac{1}{J_H\lambda}\cos\frac{k_2}{2}, \quad (60)$$

and where $\Sigma^{(2)'}_{\mu_0,k_2}$ is related with $\Sigma^{(2)}_{\mu_0,k_2}$ by a similarity transformation,

$$\Sigma^{(2)'}_{\mu_0,k_2}=\gamma^{-1}\Sigma^{(2)}_{\mu_0,k_2}\gamma. \quad (61)$$

The fact that $\Sigma^{(2)}_{\mu_0,k_2}$ is defective means that we cannot find a non-singular matrix $\beta^{(2)}_{\mu_0,k_2}$ that anticommutes with $\Sigma^{(2)}_{\mu_0,k_2}$ eventhough its spectrum is chiral. This is however not a big complication because the non-diagonal entries in $\Sigma^{(2)'}_{\mu_0,k_2}$ do not affect the determinant of $(1+\Sigma^{(2)'}_{\mu_0,k_2})$ which is important for the proof. Hence we can replace $\Sigma^{(2)}_{\mu_0,k_2}$ by a new operator $\bar{\Sigma}^{(2)}_{\mu_0,k_2}$ whose form in the basis given by γ is purely diagonal and is identical to $\Sigma^{(2)'}_{\mu_0,k_2}$ without non-diagonal entries. For this oparator one can find an anticommuting and non-singular partner and thus the proof is complete.

D. Topological invariants

To calculate the topological invariants we use an approach based on Green's function [63, 64]. Namely, we define the Green's operator $\mathcal{G}$ as,

$$\mathcal{G}(\omega,k)=\frac{1}{i\omega-\mathcal{H}_{\vec{k}}}, \quad (62)$$

where the Fermi energy is at $\omega=0$. For the non-chiral case of a Fermi surface with a codimension p, being the difference of the system's dimension d and that one of the Fermi surface d_{FS}, the topological number N_p can be expressed as an integral over an oriented manifold of the dimension p, e.g. a p-sphere, in a $(\omega,\vec{k})$-space enclosing the Fermi surface,

$$N_p=C_p\int_{S^p}\mathbf{tr}\left[\left(\mathcal{G}\mathrm{d}\mathcal{G}^{-1}\right)^p\right], \quad (63)$$

where the prefactor C_p is given by

$$C_p=-\frac{n!}{(2n+1)!(2\pi i)^{n+1}}, \quad (64)$$

with $p=2n+1$. Thus the formula is valid only for odd p and for even ones the Z topological number vanishes. Note that the power under the trace means an external product of p copies of $(\mathcal{G}\mathrm{d}\mathcal{G}^{-1})$. This formula is used to calculate the topological number (charge) of a line Fermi surface within the AI class. Because the problem is two-dimensional we have $p=1$ and thus we can get a non-vanishing N_p calculating the integral over a circle around the Fermi line. For simplicity the circle can be chosen in the (ω,k_1)-plane with a center belonging to the Fermi surface.

In the presence of a chiral symmetry $\mathcal{S}$, the Z topological number lives only at $\omega=0$ so the effective dimension

of the integration is reduced by 1. Consequently, the chiral Z topological number ν_p for the Fermi surface with a codimension p is defined by,

$$\nu_p = \frac{C_{p-1}}{2}\int_{S^{p-1}} \mathbf{tr}\left[\mathcal{S}\left(\mathcal{H}^{-1}\mathrm{d}\mathcal{H}\right)^{p-1}\right], \qquad (65)$$

where the sphere S^{p-1} is only in the $\vec{k}$-space. From this formula we can calculate the winding numbers of the chiral Dirac points within the BDI class.

Finally, we also use the Z_2 topological numbers of the first generation - $Z_2^{(1)}$. These numbers are defined by similar integrals as the Z-numbers but they require an extension of the Hamiltonian (or the Green's function). This extension involves an auxiliary parameter $u \in [0,1]$ which becomes an extra dimension to integrate over. The extended Hamiltonian has a form $\tilde{\mathcal{H}}_{\vec{k}} = (1-u)\mathcal{H}_{\vec{k}} + u\mathcal{H}_0$, where $\mathcal{H}_0$ is a trivial Hamiltonian with energies $\pm E_0$. From the extended Hamiltonian $\tilde{\mathcal{H}}$ we deduce the Green's function $\tilde{\mathcal{G}}$. The $Z_2^{(1)}$ topological number $N_p^{(1)}$ of the Fermi surface with codimension p is then given by

$$N_p^{(1)} = C_p^{'}\int_{S^p}\int_0^1 \mathrm{d}u\ \mathbf{tr}\left[\left(\tilde{\mathcal{G}}\mathrm{d}\tilde{\mathcal{G}}^{-1}\right)^p \tilde{\mathcal{G}}\partial_u\tilde{\mathcal{G}}^{-1}\right] \bmod 2, \qquad (66)$$

with a prefactor,

$$C_p^{'} = -\frac{2(p/2)!}{p!(2\pi i)^{p/2+1}}. \qquad (67)$$

Thus, the $Z_2^{(1)}$- number is non-vanishing only for even codimension p. In our case we use this formula to calculate the topological charges of the Dirac points in two dimensions- $p = 2$ within an effective D class. It is worth to mention that in this case, when we deal with a purely real 2×2 Hamiltonian, the extension $\mathcal{H}_0$ must be chosen as imaginary to get a non-vanishing $N_p^{(1)}$ - here we chose $\mathcal{H}_0 = \sigma^y$. In the end, we also need a chiral version of the $N_p^{(1)}$ invariant, namely the chiral $Z_2^{(1)}$- number $\nu_p^{(1)}$. This is defined in a usual way by

$$\nu_p^{(1)} = \frac{C_{p-1}^{'}}{2}\int_{S^{p-1}}\int_0^1 \mathrm{d}u\ \mathbf{tr}\left[\mathcal{S}\left(\tilde{\mathcal{H}}^{-1}\mathrm{d}\tilde{\mathcal{H}}\right)^{p-1}\tilde{\mathcal{H}}^{-1}\partial_u\tilde{\mathcal{H}}\right] \bmod 2. \qquad (68)$$

Such an invariant are used to characterize the Dirac points in the one-dimensional cut in the BZ.

[1] M. Z. Hasan and C. L. Kane, Rev. Mod. Phys. **82**, 3045 (2010).
[2] X.-L. Qi and S.-C. Zhang, Rev. Mod. Phys. **83**, 1057 (2011).
[3] C.-K. Chiu, J. C. Y. Teo, A. P. Schnyder, and S. Ryu, arXiv: 1505.03535v2.
[4] H. M. Weng, R. Yu, X. Hu, X. Dai, and Z. Fang, Adv. Phys. **64**, 227 (2015).
[5] C. L. Kane and E. J. Mele, Phys. Rev. Lett. **95**, 146802 (2005).
[6] B. A. Bernevig, T. L. Hughes, and S.-C. Zhang, Science **314**, 1757 (2006).
[7] J. E. Moore and L. Balents, Phys. Rev. B 75, **121306** (2007).
[8] L. Fu, C. L. Kane, and E. J. Mele, Phys. Rev. Lett. **98**, 106803 (2007).
[9] M. König *et al.* Science **318**, 766 (2007).
[10] D. Hsieh *et al.* Nature **452**, 970 (2008).
[11] Y. Xia *et al.* Nature Phys. **5**, 398 (2009).
[12] G. E. Volovik, *The Universe in a Helium Droplet* (Clarendon, Oxford, 2003).
[13] G. E. Volovik, Lect. Notes Phys. **718**, 31 (2007).
[14] X. Wan, A. M. Turner, A. Vishwanath, and S. Y. Savrasov, Phys. Rev. B **83**, 205101 (2011).
[15] T. Heikkilä and G. E. Volovik, JETP Lett. **93**, 59 (2011).
[16] K.-Y. Yang, Y.-M. Lu, and Y. Ran, Phys. Rev. B **84**, 075129 (2011).
[17] A. A. Burkov and L. Balents, Phys. Rev. Lett. **107**, 127205 (2011).
[18] W. Witczak-Krempa and Y.-B. Kim, Phys. Rev. B **85**, 045124 (2012).
[19] G. Xu, H. Weng, Z. Wang, X. Dai, and Z. Fang, Phys. Rev. Lett. **107**, 186806 (2011).
[20] G. B. Halász and L. Balents, Phys. Rev. B **85**, 035103 (2012)
[21] H. Weng, C. Fang, Z. Fang, B. A. Bernevig, and X. Dai, Phys. Rev. X **5**, 011029 (2015).
[22] S.-M. Huang, S.-Y. Xu, I. Belopolski, C.-C. Lee, G. Chang, B. Wang, N. Alidoust, G. Bian, M. Neupane, C. Zhang, S. Jia, A. Bansil, H. Lin, and M. Z. Hasan, Nat. Commun. **6**, 7373 (2015).
[23] S.-Y. Xu et al., Science **349**, 613 (2015).
[24] B. Q. Lv, H.M. Weng, B. B. Fu, X. P. Wang, H. Miao, J. Ma, P. Richard, X. C. Huang, L. X. Zhao, G. F. Chen, Z. Fang, X. Dai, T. Qian, and H. Ding, Phys. Rev. X **5**, 031013 (2015).
[25] B. Q. Lv, N. Xu, H. M. Weng, J. Z. Ma, P. Richard, X. C. Huang, L. X. Zhao, G. F. Chen, C. E. Matt, F. Bisti, V. N. Strocov, J. Mesot, Z. Fang, X. Dai, T. Qian, M. Shi, and H. Ding, Nat. Phys. **11**, 724 (2015).
[26] S.-Y. Xu, C. Liu, S. K. Kushwaha, R. Sankar, J.W. Krizan, I. Belopolski, M. Neupane, G. Bian, N. Alidoust, T.-R. Chang, H.-T. Jeng, C.-Y. Huang, W.-F. Tsai, H. Lin, P. P. Shibayev, F.-C. Chou, R. J. Cava, and M. Z. Hasan, Science **347**, 294 (2015).
[27] W. Brzezicki, C. Noce, A. Romano, and M. Cuoco, Phys. Rev. Lett. **114**, 247002 (2015).
[28] C. J. Bradley and A. P. Cracknell, The Mathematical Theory of Symmetry in Solids (Clarendon Press, Oxford, 1972).
[29] Y. Tokura, Rep. Prog. Phys. **69**, 797 (2006).
[30] A. Muñoz, M. T. Casáis, J. A. Alonso, M. J. Martínez-Lope, J. L. Martínez, and M. T. Fernández-Díaz, Inorg. Chem. **40**, 1020 (2001).

[31] S. Dong, J.-M. Liu, S.W. Cheong, and Z. F. Ren, Adv. Phys. **64**, 519 (2015).

[32] J.E. Ortmann, J.Y. Liu, J. Hu, M. Zhu, J. Peng, M. Matsuda, X. Ke, and Z.Q. Mao, Scientific Reports **3**, 2950 (2013).

[33] R. Mathieu, A. Asamitsu, Y. Kaneko, J. P. He, X. Z. Yu, R. Kumai, Y. Onose, N. Takeshita, T. Arima, H. Takagi, and Y. Tokura, Phys. Rev. B **72**, 092404 (2005).

[34] M.A. Hossain et al., Phys. Rev. B 86, 041102(R) (2012).

[35] D. Mesa, F. Ye, S. Chi, J.A. Fernandez-Baca, W. Tian, B. Hu, R. Jin, E. W. Plummer, and J. Zhang, Phys. Rev. B **85**, 180410(R) (2012).

[36] Y. Xia, D. Qian, L. Wray, D. Hsieh, G. F. Chen, J. L. Luo, N. L. Wang, M. Z. Hasan, Phys. Rev. Lett. **103**, 037002 (2009).

[37] G. F. Chen, Z. G. Chen, J. Dong, W. Z. Hu, G. Li, X. D. Zhang, P. Zheng, J. L. Luo, and N. L. Wang, Phys. Rev. B **79**, 140509(R) (2009).

[38] D. Fobes, I.A. Zaliznyak, Z. Xu, R. Zhong, G. Gu, J.M. Tranquada, L. Harriger, D. Singh, V.O. Garlea, M. Lumsden, B. Winn, Phys. Rev. Lett. **112**, 187202 (2014).

[39] F. Ye, S. Chi, H. Cao, B. C. Chakoumakos, J. A. Fernandez-Baca, R. Custelcean, T. Qi, O. Korneta, and G. Cao, Phys. Rev. B **85**, 180403 (2012).

[40] S. K. Choi, R. Coldea, A. N. Kolmogorov, T. Lancaster, I. I. Mazin, S. J. Blundell, P. G. Radaelli, Y. Singh, P. Gegenwart, K. R. Choi, S.-W. Cheong, P. J. Baker, C. Stock, and J. Taylor, Phys. Rev. Lett. **108**, 127204 (2012).

[41] J.L.García-Muñoz, J. Rodríguez-Carvajal, and P. Lacorre, Phys. Rev. B **50**, 978 (1994).

[42] J. A. Alonso *et al.*, Phys. Rev. Lett. **82**, 3871 (1999).

[43] M. T. Fernández-Díaz *et al.*, Phys. Rev. B **64**, 144417 (2001).

[44] J.-S. Zhou, J. B. Goodenough, and B. Dabrowski, Phys. Rev. Lett. **95**, 127204 (2005).

[45] R. S. K. Mong, A. M. Essin, and J. E. Moore, Phys. Rev. B **81**, 245209 (2010).

[46] C.-X. Liu, R.-X. Zhang, and B. K. VanLeeuwen, Phys. Rev. B **90**, 085304 (2014).

[47] C. Fang and L. Fu, Phys. Rev. B **91**, 161105 (2015).

[48] K. Shiozaki, M. Sato, and K. Gomi, Phys. Rev. B **91**, 155120 (2015).

[49] X.-Y. Dong and C.-X. Liu, Phys. Rev. B **93**, 045429 (2016).

[50] Q.-Z. Wang and C.-X. Liu, Phys. Rev. B **93**, 020505 (2016).

[51] D. Varjas, F. de Juan, and Y.-M. Lu, Phys. Rev. B **92**, 195116 (2015).

[52] S. Sahoo, Z. Zhang, and J. C. Y. Teo, arXiv:1509.07133 (2015).

[53] L. Lu, C. Fang, L. Fu, S. G. Johnson, J. D. Joannopoulos, and M. Soljačić, Nat. Phys. **12**, 337 (2016).

[54] K. Shiozaki, M. Sato, and K. Gomi, Phys. Rev. B **93**, 195413 (2016).

[55] S. A. Parameswaran, A. M. Turner, D. P. Arovas, and A. Vishwanath, Nat. Phys. 9, 299 (2013).

[56] Z. Wang, A. Alexandradinata, R. J. Cava, and B. A. Bernevig, Nature (London) **532**, 189 (2016).

[57] T. Bzduşek, Q. Wu, A. Rüegg, M. Sigrist, and A. A. Soluyanov, arXiv:1604.03112.

[58] B J. Wieder, Y. Kim, A. M. Rappe, and C. L. Kane, Phys. Rev. Lett. **116**, 186402 (2016).

[59] B. Bradlyn, J. Cano, Z. Wang, M. G. Vergniory, C. Felser, R. J. Cava, and B. A. Bernevig, arXiv:1603.03093.

[60] Y. Chen, H.-S. Kim, and H.-Y. Kim, Phys. Rev. B **93**, 155140 (2016).

[61] In the Appendix we present the structure and the symmetry of the model Hamiltonian for different zig-zag magnetic patterns. We provide details of the non-unitary transformation that set the determinant equivalence of the glide blocks and of the calculation of the topological invariants.

[62] C.-K. Chiu and A. Schnyder, Phys. Rev. B **90**, 205136 (2014).

[63] Y.X. Zhao and Z.D. Wang, Phys. Rev. Lett. **110**, 240404 (2013).

[64] Y.X. Zhao and Z.D. Wang, Phys. Rev. B **89**, 075111 (2014)

[65] A. Alexandradinata, Xi Dai, and B. Andrei Bernevig, Phys. Rev. B **89**, 155114 (2014)

[66] For sake of completeness, a hermitian congruence is found between the blocks H^{+}_{0,k_2} and $H^{+}_{0,k_2+2\pi}$, thus meaning that in a given basis these blocks differ only by a scaling of the rows and columns entries. The scaling relation can be expressed via four positive coefficients which are functions of k_2 and their product is equal to 1. More details are reported in the Appendix.

[67] Y. li, S. Dong, and S.-P. Kou, Phys. Rev. B **93**, 085139 (2016).

[68] L. Brey and P.B. Littlewood, Phys. Rev. Lett. **95**, 117205 (2005).

[69] K. Du *et al.*, Nat. Comm. **6**, 6179 (2015).